Published in final edited form as:
Neurochem Res. 2013 December ; 38(12): . doi:10.1007/s11064-013-1183-0.

The role of *skn-1* in methylmercury-induced latent dopaminergic neurodegeneration

Ebany J. Martinez-Finley[1,2,3], **Samuel Caito**[1,2,3], **James C. Slaughter**[4], and **Michael Aschner**[1,2,5]

[1]Division of Pediatric Toxicology and Clinical Pharmacology, Vanderbilt University Medical Center, Nashville, TN

[2]Center in Molecular Toxicology, Vanderbilt University Medical Center, Nashville, TN

[3]Vanderbilt Brain Institute, Vanderbilt University Medical Center, Nashville, TN

[4]Department of Biostatistics, Vanderbilt University Medical Center, Nashville, TN

[5]Center for Molecular Neuroscience, Vanderbilt University Medical Center, Nashville, TN

Abstract

Mercury (Hg) is a persistent environmental bioaccumulative metal, with developmental exposure to methylmercury (MeHg) resulting in long-term health effects. We examined the impact of early-life exposure to MeHg and knockdown of *skn-1* on dopaminergic (DAergic) neurodegeneration in the nematode *Caenorhabditis elegans* (*C. elegans)*. SKN-1, a the major stress-activated cytoprotective transcription factors, promotes the transcription of enzymes that scavenge free radicals, synthesizes glutathione (GSH) and catalyzes reactions that increase xenobiotic excretion. Deletions or mutations in this gene suppress stress resistance. Thus, we hypothesized that the extent of MeHg's toxicity is dependent on intact *skn-1* response; therefore *skn-1* knockout (KO) worms would show heightened sensitivity to MeHg-induced toxicity compared to wildtype worms. In this study we identified the impact of early-life MeHg exposure on Hg content, stress reactivity and DAergic neurodegeneration in wildtype, and *skn-1*KO *C. elegans.* Hg content, measured by Inductively Coupled Plasma Mass Spectrometry (ICP-MS), showed no strain-dependent differences. Reactive oxygen species (ROS) generation was dramatically increased in *skn-1*KO compared to wildtype worms. Structural integrity of DAergic neurons was microscopically assessed by visualization of fluorescently-labeled neurons, and revealed loss of neurons in *skn-1*KO and MeHg exposed worms compared to wildtype controls. Dopamine levels detected by High-performance liquid chromatography (HPLC), were decreased in response to MeHg exposure and decreased in *skn-1*KO worms, and functional behavioral assays showed similar findings. Combined, these studies suggest that knockdown of *skn-1* in the nematode increases DAergic sensitivity to MeHg exposure following a period of latency.

Keywords

Methylmercury; skn-1; early-life exposure; NRF2; DAergic neurodegeneration

Contact Information: Michael Aschner, PhD, Vanderbilt University Medical Center, Division of Pediatric Toxicology, 11425 MRB IV, 2215-B Garland Ave., Nashville, TN 37232-0414, Tel: 615-322-8024, michael.aschner@vanderbilt.edu.

INTRODUCTION

Methylmercury (MeHg) neurotoxicity has been studied for decades, but the precise molecular mechanism underlying MeHg-induced damage remains elusive. Nuclear factor erythroid 2-related factor (Nrf2) is an important mammalian stress/antioxidant response mediator. Previous studies in our laboratory have shown the upregulation of genes under the control of Nrf2 following MeHg exposure [1]. In *C. elegans* these stress responses are mediated by *skn-1*. Inhibition of *skn-1* leads to increased sensitivity to stress and deletions or loss-of-function mutations of *skn-1* suppress oxidative stress resistance [2–5]. *SKN-1* is expressed in the ASI neurons and the gut, as well as in dopaminergic (DAergic) neurons [2, 3]. Due to its involvement in the stress response and its expression pattern, *SKN-1* is posited to be an important mediator of MeHg's toxicity and of dopaminergic (DAergic) loss in neurodegenerative disease [5, 6].

Oxidative stress and lipid peroxidation represent key mechanisms in mediating neuronal death both in neurodegenerative diseases and upon exposure to MeHg [1, 7–11]. Mitochondrial damage is implicated in the loss of DAergic neurons in Parkinson's disease (PD), corroborated by findings that mitochondrial poisons, such as 1-methyl-4-phenyl-1,2,3,6-tetrahydropyridine (MPTP), rotenone and 6-hydroxydopamine induce a Parkinsonian-like syndrome [12–15]. Post-mortem PD brains show increased levels of lipid peroxidation, protein oxidation, 3-nitrotyrosine formation, DNA oxidation and breaks, and a decrease in the activities of reactive oxygen species (ROS) scavenging enzymes and glutathione (GSH) peroxidase [16–19]. Combined, there is ample evidence to suggest that MeHg and PD share common molecular mechanisms of DAergic degeneration, including mitochondrial dysfunction, oxidative damage, GSH depletion and -synuclein aggregation [10, 12, 20–24].

Developmental exposure to MeHg has long-term, latent health effects [25–31]. Early-life exposure may remain silent for decades and become unmasked late in life by aging and genetic predisposition [32]. In this study we focused on the role of *skn-1* in mediating the late-life occurrence of DAergic neurodegeneration following early-life MeHg exposure, positing heightened DAergic neurodegeneration in *skn-1*KO compared to wildtype worms. Our studies examined DAergic function, structural integrity and dopamine (DA) levels following knockdown of *skn-1* and exposure to MeHg.

MATERIALS AND METHODS

1.1 C. elegans maintenance

C. elegans strains were handled and maintained at 20°C as previously described [33]. Worms were grown on plates containing nematode growth medium (NGM) or 8P and seeded with either *Escherichia coli* strain OP50 or NA22, respectively, as previously described [33]. The following strains were used: N2 Bristol (wildtype) strain (as a control for all experiments), VC1772 (skn-1(ok2315) IV/nT1[qIs51](IV;V)) strain (referred to as *skn-1*KO in all experiments), LG326 (skn-1(zu169) IV; geIs7) and *cat-2* mutants (TH deficient). Because *skn-1* is required for optimal worm development, and exposure to MeHg was carried out at the L1 stage (early lifespan), worms with a homozygous deletion could not be used. The homozygous deletion is lethal, while the VC1772 strain has a heterozygous deletion with a balancer to yield surviving larva. All strains were obtained from the *Caenorhabditis* Genetics Center, Minneapolis, MN.

1.2 MeHgCl exposure

To obtain a synchronous population prior to exposure, worms were treated with an alkaline bleach solution. Methylmercuric chloride (CH_3HgCl; Sigma-Aldrich) exposures (0–50μM) were performed for 30 minutes (min) in synchronized L1 worms to determine appropriate dosing. Five thousand (lifespan, lethality, and behavior), 10,000 (DCF assay), 20,000 (RNA), 50,000 (ICP-MS) or 150,000 (dopamine) nematodes were treated with 0 or 20μM MeHgCl. After exposure, worms were washed three times with M9 buffer (KH_2PO_4; Na_2HPO_4; and NaCl) and either plated on seeded NGM plates or collected for immediate analysis. A sample size of six (n = 6) represents the total number of independent worm preparations; each independent experiment was carried out with 5,000–150,000 worms (see above).

1.3 Lethality

Following exposure and washing, 5,000 worms were plated on seeded 60 mm NGM plates and allowed to grow for 24 hours (hrs). Worms were then counted and scored using a grid system. Nematodes on 4 of the 64 grids were counted and the number of worms per grid was averaged and multiplied by 64. Surviving worms were expressed as percent control.

1.4 Lifespan

For lifespan determination, 40 nematodes from each dose group were picked to a fresh NGM plate 24 hrs following exposure. The worms were counted each day and scored as live or dead (worms were censored if dead bodies could not be located). Live *C. elegans* were picked to new plates each day during the egg-laying period of their lifecycle; once egg-laying ceased they were picked every other day until no live *C. elegans* remained.

1.5 Inductively Coupled Plasma-Mass Spectrometry (ICP-MS) for Mercury content

The protocol used for ICP-MS was carried out as previously described [33]. Briefly, 50,000 worms were treated with MeHgCl, then washed three times with M9. Samples were then air-dried until a dehydrated pellet was obtained. Next, the dried sample was transferred to pre-weighed Teflon jars and reweighed. Concentrated acids HNO_3, HCl and H_2SO_4 were added, and the samples were placed overnight in heat block at 100°C under the fume hood. The following day, digested samples were reweighed and placed in pre-weighed metal-free 15mL centrifuge tubes. They were analyzed by ICP-MS with a Hg limit-of-detection in the parts per trillion range.

1.6 DCF assay for oxidative stress

Synchronized L1s were treated with MeHg as described earlier, and washed in M9 buffer. The formation of reactive oxygen species (ROS) was evaluated with 6-carboxy-2′,7′-dichlorodihydrofluorescein diacetate at 1 mM for one hr in the dark. The worms were then washed in M9, 4 additional times. The supernatants were transferred to a 96-well plate and their fluorescence levels (excitation: 485 nm; emission: 535 nm) detected with a FLEXstation III (Molecular Devices) pre-heated to 37°C. Fluorescence in each well was measured at time 0 and 1 hr after the addition of MeHg. Values from all readings were adjusted for background signal and reported as percent fluorescence relative to their respective control strain.

1.7 mRNA isolation

Following MeHg exposure, 20,000 synchronized L1 stage worms were washed 3 times with M9 and frozen at −80°C until RNA purification. Worm pellets were suspended in Trizol (200μL/100μL pellet); the protein and other impurities were separated from nucleic acids

with chloroform. The pellets were washed with 70% EtOH; DNA was digested with RNAse free DNAse kit (Ambion). RNA concentrations were determined with a ND-1000 spectrophotometer (NanoDrop®; OD 260nm).

1.8 cDNA synthesis

Reverse transcription reactions were performed in 20 μL following the manufacturer's protocol (Applied Biosystems). A 10μL reaction mixture containing 10X RT buffer, 25X dNTP mix (100mM), 10X random primers, Multiscribe reverse transcriptase and sterile nuclease-free water was added to 10μL of RNA (75ng). The contents were mixed gently and incubated at 25°C for 10 min, 37°C for 120 min followed by inactivation by heating at 85°C for 5 min. Synthesized cDNA was stored at −20°C.

1.9 Semi-quantitative determination of transcript levels by Real-time PCR

Real-time PCR was conducted in a Gene Amp 7300 sequence detection system (Applied Biosystems) in a 96-well plate (MicroAmp™ Fast). The relative quantification was determined with the $2^{-\Delta\Delta Ct}$ method [34]. *gpd-1* (mammalian:GAPDH) was used as an internal control. Oligonucleotide sequences for *skn-1*: 5′AGTGTCGGCGTTCCAGATTTC3′ and 5′GTCGACGAATCTTGCGAATCA3′; *gst-4*: 5′TGCTCAATGTGCCTTACGAG3′ and 5′AGTTTTTCCAGCGAGTCCAA3′; *gpd-1* (housekeeping): 5′CAATGCTTCCTGCACCACTA3′ and 5′CTCCAGAGCTTTCCTGATGG3′. The specificity of each primer pair was confirmed by the identification of a single PCR product of predicted size on 1.5% (w/v) agarose gels. Oligonucleotide sequences were designed based on published literature.

1.10 Dopamine measured via High-Performance Liquid Chromotagraphy (HPLC)

One hundred fifty thousand synchronized L1 worms were collected and washed three times in M9. Next, they were pelleted and the supernatant removed. Tubes were immediately frozen in liquid nitrogen and stored at −80°C. For each tube, the worm pellet was re-suspended in lysis buffer containing EDTA to scavenge free metal ions and then sonicated to disrupt cell membranes. A portion of the lysate was used for protein levels and analyzed via bicinchoninic acid (BCA) assay. Isoproterenol, dihydroxybenzylamine (internal standard), Tris buffer and Al_2O_3 was added to the remaining lysate, which was applied to the alumina to bind DA. After 30 min, the buffer was removed and the Al_2O_3 was washed three times with water. Next, the alumina was eluted with 0.1 acetic acid and the collected samples were injected into the biogenic amine HPLC chromatograph. To correct for inter-sample variations in the extraction efficiency, the ratio of DA to isoproternol was estimated, and the total DA content calculated relative to protein levels.

1.11 Basal slowing behavioral analysis

The behavioral analysis was adapted from a previously published protocol [35]. Well-fed L4 worms from the same exposure group were placed on two sets of 60×15mm plates: one with ~20μL bacteria spread in a ring with an inner diameter of ~1cm and an outer diameter of ~3.5cm and one without bacteria (both incubated at 37°C overnight and cooled to room temperature prior to assay). Bacterial mechanosensation induces the dopamine-mediated slowing of locomotion in the presence of food (bacteria) and can be measured by counting the number of body bends per 20-second interval. Locomotor rates were compared between well-fed worms placed on plates of food versus those placed on plates in the absence of food; this ratio is referred to as the change (Δ) in body bends/20 seconds. A lower value represents diminished slowing on food, indicating deficits in DAergic function. The *cat-2* strain is tyrosine hydroxylase (TH) deficient and therefore defective in bacterial mechanosensation, representing a positive control [35].

1.12 Microscopy

To examine *skn-1* protein expression, 10–15 worms in M9 were mounted on 4% agarose pads and anaesthetized with 0.2% tricaine/0.02% tetramisole in M9. *skn-1*::GFP (LG326) worms were selected by fluorescence microscopy 24–48 hrs following exposure. Fluorescence was determined with an epifluorescence microscope (Nikon Eclipse 80i, Nikon Corporation, Tokyo, Japan) equipped with a Lambda LS Xenon lamp (Sutter Instrument Company) and Nikon Plan Fluor 20× dry and Nikon Plan Apo 60 × 1.3 oil objectives.

To examine morphological changes in neurons as a result of MeHg exposure, worms expressing $P_{dat\text{-}1}$::mCherry in DAergic neurons (N2 and VC1772) were visualized by confocal microscopy. Worms were treated with 0 or 20μM MeHg and visualized 96 hrs following exposure. Approximately 20 worms were mounted on 4% agarose pads in M9 and anaesthetized with 0.2% tricane and 0.02% tetramisole. Images were captured through Plan-Apochromat 20x objective on a LSM510 confocal microscope (Carl Zeiss MicroImaging, Inc) scanning every 200 nm for XZ sections. Images were processed with the Zeiss LSM Image Browser.

1.13 Statistical analysis

Statistics were carried out with GraphPad Prism. Briefly, we used a sigmoidal dose-response model with a top constraint at 100% to draw the curves and determine the LD_{50}. The Kaplan-Meier method was used to estimate survival curves. Curves were compared with the log rank test or Wald test of coefficients from a Cox proportional hazards regression. Statistical analysis of significance was carried out by one-way analysis of variance (ANOVA) for change in DA-mediated locomotor activity. Two-way ANOVA for dopamine, ROS, *skn-1*, *gst-4* and MeHg content. When p values in the ANOVA were <0.05, the source of the statistical difference was determined by *post-hoc* Bonferroni or student's t-test. Error bars in all the figures represent ±SEM.

RESULTS

2.1 MeHg-induced lethality (Figure 1)

To determine appropriate MeHg concentrations for dosing in our studies, N2 and *skn-1*KO *C. elegans* were treated with MeHg (0–50μM) for 30 min and counted 24 hrs later. Assessment of lethality following 30 min exposure revealed a significant leftward shift for *skn-1*KOs compared to N2 wildtype worms (**p<0.004) and a similar significant leftward shift for *skn-1*KOs compared to LG326 worms (**p<0.001). LD_{50} for N2, *skn-1* KO, and LG326 were 25, 19 and 26μM, respectively. These data suggest that *skn-1*KO worms are more sensitive to MeHg than N2 wildtypes. It is noteworthy that doses applied in the present study are of physiological relevance to mammalian systems. For example, perinatal MeHg treatment in rats resulted in observable effects with Hg concentrations at 0.1 μgHg/g brain [36], and continuous pre- and postnatal exposure in rats was associated with brain Hg concentrations of 0.5 μg/g at birth and 0.04 μg/g at weaning [37]. The threshold for observable clinical effects in humans is ~0.3μg/g [36].

2.2 Mercury content (Figure 2)

To determine if there were differences in MeHg retention mediated by *skn-1*KO, we assessed Hg content immediately following exposure. ICP-MS quantification of Hg content revealed a significant dose effect (**p=0.0003), but no strain effect (p=0.958, n.s.), or a dose x strain interaction (p=0.438, n.s.). There were no strain differences in Hg content.

2.3 Lifespan (Figure 3)

To determine long-term sensitivity to MeHg and to discern if its effect is exacerbated by KO of *skn-1*, we performed lifespan measurements. Log-rank test revealed that MeHg had a significant effect on lifespan in *skn-1*KO (*p=0.006) worms, which was not seen in wildtype worms (p=0.61). Knockout of *skn-1* alone had an effect on lifespan, which was exacerbated by exposure to MeHg (fig. 3).

2.4 Reactive oxygen species (ROS) levels are elevated in *skn-1*KO and following MeHg exposure (Figure 4)

We hypothesized that early-life exposure to MeHg would increase toxicity reflecting increased ROS production. The DCF assay showed a significant increase in ROS levels in wildtype strains immediately following (fig. 4A) and 1hr after (fig. 4B) 20μM MeHg exposure. *skn-1*KO worms had significantly increased ROS levels (compared to wildtype worms) even in the absence of MeHg exposure. A greater increase in ROS levels was noted in *skn-1*KO MeHg exposed worms compared to *skn-1*KO unexposed worms, but it did not attain statistically significance (fig. 4). ROS generation immediately upon MeHg exposure was strain- (**p=0.0002), but not dose- (p=0.468, n.s.) or dose x strain-dependent (p=0.562, n.s); at 1hr the ROS increased in all strains (strain effect **p=0.0002; dose p=0.375; dose x strain interaction p=0.504). Sodium nitroprusside (NaNP) was used as a positive control and MeHg in the absence of worms was used as a negative control (not shown). *Post-hoc* analysis showed that immediately following MeHg exposure wildtype worms exhibited significantly higher ROS levels compared to unexposed wildtype controls (*p=0.04). Both untreated and treated *skn-1*KO worms (**p=0.0012;*p=0.018, respectively) had significantly increased ROS levels compared to wildtype untreated worms. *skn-1*KO treated worms were not significantly different from their respective untreated controls (p=0.5262, n.s.). One hour after MeHg exposure, wildtype worms exhibited significantly higher ROS levels compared to unexposed wiltype controls (*p=0.04). Both untreated and treated *skn-1*KO worms (***p=0.0001;*p=0.02, respectively) had significantly higher ROS levels compared to wildtype untreated, and *skn-1*KO treated worms were not significantly different from their respective untreated controls (p=0.4517, n.s.). Collectively, this data suggests that *skn-1* plays an important role in mitigating oxidative stress even under basal conditions and in the absence of MeHg exposure.

2.5 MeHg induces *SKN-1*-mediated increase in Phase II detoxification genes (Supplemental Figure 1)

skn-1-regulated genes were assessed to validate knockdown of *skn-1* and activation of *skn-1* in wildtype MeHg exposed worms. Whole extracts were used to probe for *skn-1* and *gst-4* transcriptional activity. Using qRT-PCR, we show that wildtype worms significantly upregulate *skn-1* (*p<0.05; supplemental fig. 1A) and *gst-4* mRNA levels (*p<0.05; supplemental fig. 1B) in response to MeHg, but *skn-1*KO worms do not. Differences in the average threshold cycle (ΔCt) were determined and normalized to the expression of *gpd-1*. These data suggest that wildtype worms mounted an *skn-1*-mediated antioxidant response, whereas *skn-1*KO worms failed to do so in response to MeHg. Analysis of *skn-1* mRNA, revealed a significant strain (**p=0.002), and dose effect (**p=0.002), but not a dose x strain interaction (supplemental fig. 1A). *gst-4* mRNA analysis showed a significant dose effect (***p=0.0007), strain effect (***p=0.001) and a dose x strain interaction (**p=0.007) (supplemental fig 1B). *Post-hoc* analysis showed *skn-1* levels were significantly induced in wildtype worms following MeHg exposure (**p=0.003) but not in *skn-1*KO worms. There was a significant difference in *skn-1* mRNA between the strains in 0 μM control worms (**p=0.003). *skn-1* mRNA levels in wildtype 20 μM MeHg versus *skn-1*KO 20 μM MeHg were significantly different (^p=0.02). *Post-hoc* for *gst4* mRNA levels showed that wildtype

0 μM MeHg was significantly different from wildtype 20 μM MeHg (**p=0.001) and from *skn-1*KO 0μM MeHg (**p=0.002). There was also a significant difference between N2 20μM and *skn-1*KO 20μM MeHg exposed worms (^p=0.01). This data showed that optimal stress responsiveness was absent in our *skn-1*KO worms.

2.6 *skn-1* is induced 24 hrs after exposure to MeHg (Figure 5)

Intestinal accumulation of *skn-1* in *C. elegans* is apparent following 20 μM MeHg exposure, this accumulation was absent in 0 and 10μM MeHg exposed worms. SKN-1 is present in ASI nuclei under normal conditions, and accumulates in intestinal nuclei in response to oxidative stress (An and Blackwell, 2003). The accumulation of *skn-1* in the intestine of worms exposed to 20μM MeHg suggests activation of *skn-1* is occurring in response to sublethal doses of MeHg.

2.7 DA content (Figure 6)

Prenatal MeHg exposure studies in animals have described altered DAergic function [38, 39]. Accordingly, we examined the extent of DAergic neurodegeneration in response to early-life MeHg exposure. Worms' DA levels were determined immediately after MeHg exposure, when the worms were at the L1 stage. DA levels were correlated to the DA-mediated behavioral data which was collected 72 hrs post exposure (fig. 7) and the structural data collected at 96 hrs post exposure (fig. 8). There was no significant effect of dose ($p=0.51$); or dose x strain interaction ($p=0.11$), there was a significant strain effect (**$p<0.005$). There was a trend towards decreased DA content in MeHg exposed N2 wildtype worms, and no significant difference in *skn-1*KO worms. These findings corroborate the functional behavioral DA readout, which was measured 72 hrs following exposure (fig. 6). *Post-hoc* analyses revealed a significant difference between the 0 μM MeHg wildtype worms and all other strains/doses (*$p<0.05$;**$p<0.005$; ***$p<0.0001$). DA content from treated and untreated wildtype and *skn-1*KO worms were significantly different from *cat2* mutants.

2.8 Basal slowing behavioral analysis (Figure 7)

We analyzed DA-mediated behavior 72 hrs post exposure (adult stage) to determine if there was a decrease in functional DA. For each strain, locomotion rates in the absence and presence of bacteria (supplemental fig. 2) were calculated, and results are presented as change (Δ) body bends/20 seconds (fig. 8). Higher values indicate functional, while lower values indicate dysfunctional DAergic neurons. When the change in locomotor activity (Δ body bends/20 seconds) was compared by one-way ANOVA, it was statistically significant (***$p<0.0001$). *Post-hoc* analysis showed all doses/strains were significantly different from 0 μM MeHg wildtype (*$p<0.05$, ***$p<0.0005$) and all doses/strains were significantly different from 0 μM MeHg *skn-1*KOs ($^{\#}p<0.05$). *cat-2* mutants unexposed worms were significantly different from all MeHg-treated wildtype worms (*$p<0.05$).

2.9 Degeneration and loss of fluorescence in *skn-1KO* DAergic neurons after low dose MeHg exposure (Figure 8)

We assessed the structural integrity of mCherry-labeled DAergic neurons in wildtype and *skn-1*KO worms, 96 hrs after MeHg exposure. MeHg exposed wildtype worms showed loss of fluorescence similar to *skn-1*KO worms. In *skn-1*KO MeHg exposed worms, the loss of fluorescence was exacerbated compared to *skn-1*KO unexposed worms and wildtype MeHg exposed worms. This data suggests that *skn-1*KO worms are susceptible to DAergic neurodegeneration following short, early life exposure to MeHg. CEP: cephalic, ADE: anterior deirid DAergic neurons.

DISCUSSION

MeHg is an environmental contaminant of concern due to its widespread release and contamination of fish [40, 41]. The nervous system is the primary target of MeHg and environmental exposure, particularly in fish-eating populations, can be detrimental. While adults are susceptible to MeHg exposure, the developmental period in humans and rodents is a window of high vulnerability [42, 43] and perinatal exposure to MeHg presents with a less specific pattern of damage than that of adult exposure, shown to by concentration-, duration of exposure- and stage of development-dependent [44]. Latent effects following MeHg exposure have also been described [29]. Therefore, it is important to address the effects of early life exposure to MeHg on later life endpoints like neurodegeneration. Our findings revealed that early-life MeHg exposure led to decreases in DA-mediated behavior seen at 72 hrs which positively correlated to DAergic degeneration at 96 hrs (adult life stage).

MeHg is known to produce oxidative stress and the *skn-1* (Nrf2 homolog) signaling pathway is involved in oxidative stress resistance and eradication of oxidants [1, 4, 45–48]. Given that oxidative stress mediates both MeHg toxicity and the development of PD [10, 12, 20, 23, 24], we assessed the role of *skn-1* in MeHg-induced oxidative stress response and its contribution to DAergic toxicity. While other neuronal subtypes are also susceptible to MeHg, emphasis was directed to DAergic neurons based on their expression of *skn-1* [3] and the documented importance of *skn-1* in attenuating MeHg toxicity [1]. We focused on addressing whether MeHg exposures that occur early in the lifespan have deleterious effects later in life.

Assessment of lethality 24 hrs after 30 min exposure to MeHg during the L1 period indicated that *skn-1*KO worms are more sensitive to MeHg exposure (fig. 1). This heightened sensitivity is likely not due to increased uptake of Hg in *skn-1*KO worms as there were no strain differences in Hg content immediately after exposure (fig. 2).

Lifespan was significantly affected by MeHg exposure in both the wildtype and *skn-1*KO strains. Consistent with other published studies, *skn-1*KOs had a significant decrease in lifespan compared to wildtype worms (fig. 3) [2]; this decrease was further exacerbated by MeHg exposure. Many environmental contaminants have a significant impact on lifespan through generation of ROS [49–53]. The increase in ROS levels following MeHg exposure is consistent with earlier reports [10]. More striking is the increased ROS production measured in the *skn-1*KO untreated strain compared to the untreated wildtype strain. This increase at baseline has been documented in the human cell-line and murine literature following silencing or knockdown of Nrf2 [54, 55] suggesting that *skn-1* is important in regulating ROS levels under basal conditions as well as after presentation of a stimulus.

skn-1 knockdown was confirmed by measuring RNA content (supplemental fig. 1A) for *skn-1* and *gst-4*, a gene under the control of *skn-1* (supplemental fig. 1B). *skn-1* and *gst-4* levels increased following MeHg exposure in wildtype worms, but did not increase in *skn-1*KO worms, confirming the knockdown (supplemental fig. 1A/B). *skn-1*::GFP worms assessed at 24 hrs showed gut florescence in the 20μM MeHg exposed worms, indicating activation of *skn-1* (fig. 5). SKN-1 is present in ASI nuclei under normal conditions, and accumulates in intestinal nuclei in response to oxidative stress [2]. Under basal conditions, glycogen synthase kinase 3 (gsk3; mammalian: Keap1) inhibits *skn-1* nuclear localization [56]. Following oxidative stress, *skn-1* is liberated from gsk3 repression and translocates to the nucleus, leading to transcription of Phase II detoxification genes [57]. Inhibition of *skn-1* leads to increased sensitivity to stress [2].

Our studies were designed to establish novel and translational information on mechanisms associated with DAergic neurodegeneration, especially after early life exposure to MeHg. We are reporting the presence of irregularities in DAergic neurons 96 hrs following 30 min exposure (at L1 stage) to 20μM MeHg (fig. 8). *C. elegans* possess eight DAergic neurons; four cephalic (CEP) neurons, two anterior deirid (ADE) neurons, and two postdeirid (PDE) neurons (fig. 8; PDE not shown). We show degeneration of the DAergic neurons 96 hrs following exposure to MeHg (fig. 8); however, *skn-1*KO worms show degeneration even in the absence of MeHg exposure. These results indicating loss of DAergic neurons in *skn-1*KO worms are corroborated by an Nrf2-knockout mouse model, which showed 23% greater nigral DAergic neuron loss as measured by positive stain for TH, than Nrf2+/+ mice [6]. It is not surprising that MeHg exposed *skn-1*KOs show the most robust loss in DAergic neuron integrity given the evidence for the role of Nrf2 in the DAergic system. Nrf2 induction in transgenic mice brains has been shown to be protective of MPTP damage in the nigrostriatal DAergic pathway [4] and Nrf2 has been shown to translocate to the nucleus in the substantia nigra of PD patients, although it has proved to be insufficient for protection [5]. Another fact that cannot be overlooked is that Nrf2 activity decreases with age while PD susceptibility increases with age [58]. The decrease in fluorescence in our model could be explained by decreases in DAT, as the mCherry florephore is under the control of dat-1 promoter. Another group reported decreases in total DAT activity in MeHg exposed murine embryonic stem cells as well as decreases in TH+ cells and downregulation of DA receptors [59] suggesting that the dopamine system is particularly susceptible to MeHg.

The decrease in DA in wildtype worms (fig. 6) suggests that MeHg has significant effects on DAergic neuron function. The absence of effect of MeHg on *skn-1*KO worm DA levels is interesting, given our hypothesis that *skn-1*KO worms should be more susceptible to DAergic changes following exposure (fig. 6). The lack of MeHg effect in this strain may be due to the early time point in which the DA levels were measured (i.e. immediately rather than days after exposure), not allowing time for a measureable effect. Additionally, DA metabolites may present a more complete understanding of DA vulnerability [60] but we are unable to measure DA metabolites in our model. It is known that dopamine can oxidize and form ROS and reactive quinones and that those quinones can covalently bind to cysteine sites [61]. The dopamine transporter has several cysteine residues and therefore is a target for covalent modification by reactive quinones and ROS [62]. This type of modification to DA transporters could explain the altered state of the DAergic system seen after MeHg exposure. The decreased basal levels of DA in *skn-1*KO control worms compared to wildtype controls (fig. 6) have been reported in murine literature showing low basal levels of TH immunoreactivity in $Nrf2^{-/-}$ mice [45].

The basal slowing behavior, assessed 72 hrs following exposure (fig. 7), confirms the loss of functional DAergic neurons. Functional DAergic neurons are required for food sensing (mechanosensation) [35]. This data is consistent with the images taken at 96 hrs (fig. 8) and the trends in DA levels immediately following exposure (fig. 6).

Neuronal differentiation and establishment of connectivity occurs early in the lifespan and could be disrupted by exposure to MeHg. These connections, or lack thereof, may not be apparent until the brain has completed the developmental period therefore we do not see them until after a period of latency. Acute and chronic MeHg exposures have been shown to produce latent toxicity (reviewed in [29]). Others have postulated that microtubule function may be altered by MeHg preferential binding to sulfhydryl groups [63] and this may result in altered cytoskeletal architecture, which in our studies, is described as degeneration. Another explanation for the latency period is that these effects may not be seen until after a period of normal decline due to aging thereby exposing the MeHg-induced damage to the DAergic system.

Taken together and consistent with the Barker hypothesis [64, 65], these results indicate that acute early-life exposure to MeHg confers DAergic neurodegeneration later in life. Furthermore, knockdown of *skn-1* amplifies MeHg's effect. Future studies should aim to address if Hg is still present at later time periods to determine what role, if any, they are playing in the degenerative process as well as establish a timeline of cell death of the DAergic neurons. It would also be beneficial to examine other neuronal subtypes to determine if there is additional damage.

Supplementary Material

Refer to Web version on PubMed Central for supplementary material.

Acknowledgments

This manuscript was supported by the National Institute of Environmental Health Sciences (NIEHS) [R01ES07331, T32ES007028] and the National Institutes of Health Loan Repayment Program. We would like to acknowledge the *Caenorhabditis* Genetic Center (CGC), which is funded by the NIH Office of Research Infrastructure Programs (P40 OD010440), for providing the strains used in this manuscript.

Literature Cited

1. Ni M, et al. Methylmercury induces acute oxidative stress, altering Nrf2 protein level in primary microglial cells. Toxicol Sci. 2010; 116(2):590–603. [PubMed: 20421342]
2. An JH, Blackwell TK. SKN-1 links C. elegans mesendodermal specification to a conserved oxidative stress response. Genes Dev. 2003; 17(15):1882–93. [PubMed: 12869585]
3. Vanduyn N, et al. SKN-1/Nrf2 inhibits dopamine neuron degeneration in a Caenorhabditis elegans model of methylmercury toxicity. Toxicol Sci. 2010; 118(2):613–24. [PubMed: 20855423]
4. Kaidery NA, et al. Targeting Nrf2-mediated gene transcription by extremely potent synthetic triterpenoids attenuate dopaminergic neurotoxicity in the MPTP mouse model of Parkinson's disease. Antioxid Redox Signal. 2013; 18(2):139–57. [PubMed: 22746536]
5. Ramsey CP, et al. Expression of Nrf2 in neurodegenerative diseases. J Neuropathol Exp Neurol. 2007; 66(1):75–85. [PubMed: 17204939]
6. Lastres-Becker I, et al. alpha-Synuclein expression and Nrf2 deficiency cooperate to aggravate protein aggregation, neuronal death and inflammation in early-stage Parkinson's disease. Hum Mol Genet. 2012; 21(14):3173–92. [PubMed: 22513881]
7. Gorell JM, et al. Occupational exposure to manganese, copper, lead, iron, mercury and zinc and the risk of Parkinson's disease. Neurotoxicology. 1999; 20(2–3):239–47. [PubMed: 10385887]
8. Gutteridge JM. Lipid peroxidation and antioxidants as biomarkers of tissue damage. Clin Chem. 1995; 41(12 Pt 2):1819–28. [PubMed: 7497639]
9. Recchia A, et al. Alpha-synuclein and Parkinson's disease. FASEB J. 2004; 18(6):617–26. [PubMed: 15054084]
10. Aschner M, et al. Involvement of glutamate and reactive oxygen species in methylmercury neurotoxicity. Braz J Med Biol Res. 2007; 40(3):285–91. [PubMed: 17334523]
11. Zhang P, et al. In vitro protective effects of pyrroloquinoline quinone on methylmercury-induced neurotoxicity. Environ Toxicol Pharmacol. 2009; 27(1):103–10. [PubMed: 21783927]
12. Chiueh CC, et al. In vivo generation of hydroxyl radicals and MPTP-induced dopaminergic toxicity in the basal ganglia. Ann N Y Acad Sci. 1994; 738:25–36. [PubMed: 7832434]
13. Dabbeni-Sala F, et al. Melatonin protects against 6-OHDA-induced neurotoxicity in rats: a role for mitochondrial complex I activity. FASEB J. 2001; 15(1):164–170. [PubMed: 11149904]
14. De Iuliis A, et al. A proteomic approach in the study of an animal model of Parkinson's disease. Clin Chim Acta. 2005; 357(2):202–9. [PubMed: 15946658]
15. Sherer TB, et al. Subcutaneous rotenone exposure causes highly selective dopaminergic degeneration and alpha-synuclein aggregation. Exp Neurol. 2003; 179(1):9–16. [PubMed: 12504863]

16. Riederer P, et al. Transition metals, ferritin, glutathione, and ascorbic acid in parkinsonian brains. J Neurochem. 1989; 52(2):515–20. [PubMed: 2911028]
17. Sian J, et al. Alterations in glutathione levels in Parkinson's disease and other neurodegenerative disorders affecting basal ganglia. Ann Neurol. 1994; 36(3):348–55. [PubMed: 8080242]
18. Sian J, et al. Glutathione-related enzymes in brain in Parkinson's disease. Ann Neurol. 1994; 36(3): 356–61. [PubMed: 8080243]
19. Sofic E, et al. Reduced and oxidized glutathione in the substantia nigra of patients with Parkinson's disease. Neurosci Lett. 1992; 142(2):128–30. [PubMed: 1454205]
20. Bender A, et al. High levels of mitochondrial DNA deletions in substantia nigra neurons in aging and Parkinson disease. Nat Genet. 2006; 38(5):515–7. [PubMed: 16604074]
21. Cantuti-Castelvetri I, et al. Somatic mitochondrial DNA mutations in single neurons and glia. Neurobiol Aging. 2005; 26(10):1343–55. [PubMed: 16243605]
22. Kraytsberg Y, et al. Mitochondrial DNA deletions are abundant and cause functional impairment in aged human substantia nigra neurons. Nat Genet. 2006; 38(5):518–20. [PubMed: 16604072]
23. Swerdlow RH, et al. Origin and functional consequences of the complex I defect in Parkinson's disease. Ann Neurol. 1996; 40(4):663–71. [PubMed: 8871587]
24. Gorell JM, et al. Occupational metal exposures and the risk of Parkinson's disease. Neuroepidemiology. 1999; 18(6):303–8. [PubMed: 10545782]
25. Gao Y, et al. Effects of methylmercury on postnatal neurobehavioral development in mice. Neurotoxicol Teratol. 2008; 30(6):462–7. [PubMed: 18706997]
26. Lin FM, Malaiyandi M, Sierra CR. Toxicity of methylmercury: effects on different ages of rats. Bull Environ Contam Toxicol. 1975; 14(2):140–8. [PubMed: 1174722]
27. do Maia CS, et al. Inhibitory avoidance acquisition in adult rats exposed to a combination of ethanol and methylmercury during central nervous system development. Behav Brain Res. 2010; 211(2):191–7. [PubMed: 20346984]
28. Uchino M, et al. Neurologic features of chronic Minamata disease (organic mercury poisoning) certified at autopsy. Intern Med. 1995; 34(8):744–7. [PubMed: 8563113]
29. Weiss B, Clarkson TW, Simon W. Silent latency periods in methylmercury poisoning and in neurodegenerative disease. Environ Health Perspect. 2002; 110(Suppl 5):851–4. [PubMed: 12426145]
30. Yoshida M, et al. Emergence of delayed methylmercury toxicity after perinatal exposure in metallothionein-null and wild-type C57BL mice. Environ Health Perspect. 2008; 116(6):746–51. [PubMed: 18560530]
31. Yoshida M, et al. Neurobehavioral effects of combined prenatal exposure to low-level mercury vapor and methylmercury. J Toxicol Sci. 2011; 36(1):73–80. [PubMed: 21297343]
32. Landrigan PJ, et al. Early environmental origins of neurodegenerative disease in later life. Environ Health Perspect. 2005; 113(9):1230–3. [PubMed: 16140633]
33. Helmcke KJ, et al. Characterization of the effects of methylmercury on Caenorhabditis elegans. Toxicol Appl Pharmacol. 2009; 240(2):265–72. [PubMed: 19341752]
34. Livak KJ, Schmittgen TD. Analysis of relative gene expression data using real-time quantitative PCR and the 2(−Delta Delta C(T)) Method. Methods. 2001; 25(4):402–8. [PubMed: 11846609]
35. Sawin ER, Ranganathan R, Horvitz HR. C. elegans locomotory rate is modulated by the environment through a dopaminergic pathway and by experience through a serotonergic pathway. Neuron. 2000; 26(3):619–31. [PubMed: 10896158]
36. Burbacher TM, Rodier PM, Weiss B. Methylmercury developmental neurotoxicity: a comparison of effects in humans and animals. Neurotoxicol Teratol. 1990; 12(3):191–202. [PubMed: 2196419]
37. Newland MC, Rasmussen EB. Aging unmasks adverse effects of gestational exposure to methylmercury in rats. Neurotoxicol Teratol. 2000; 22(6):819–28. [PubMed: 11120387]
38. Dare E, et al. Effects of prenatal exposure to methylmercury on dopamine-mediated locomotor activity and dopamine D2 receptor binding. Naunyn Schmiedebergs Arch Pharmacol. 2003; 367(5):500–8. [PubMed: 12684742]
39. Reed MN, Newland MC. Gestational methylmercury exposure selectively increases the sensitivity of operant behavior to cocaine. Behav Neurosci. 2009; 123(2):408–17. [PubMed: 19331463]

40. Clarkson TW, Magos L. The toxicology of mercury and its chemical compounds. Crit Rev Toxicol. 2006; 36(8):609–62. [PubMed: 16973445]
41. Clarkson TW, Magos L, Myers GJ. The toxicology of mercury--current exposures and clinical manifestations. N Engl J Med. 2003; 349(18):1731–7. [PubMed: 14585942]
42. Castoldi AF, et al. Neurodevelopmental toxicity of methylmercury: Laboratory animal data and their contribution to human risk assessment. Regul Toxicol Pharmacol. 2008; 51(2):215–29. [PubMed: 18482784]
43. Goulet S, Dore FY, Mirault ME. Neurobehavioral changes in mice chronically exposed to methylmercury during fetal and early postnatal development. Neurotoxicol Teratol. 2003; 25(3): 335–47. [PubMed: 12757830]
44. Rodier PM. Developing brain as a target of toxicity. Environ Health Perspect. 1995; 103(Suppl 6): 73–6. [PubMed: 8549496]
45. Rojo AI, et al. Nrf2 regulates microglial dynamics and neuroinflammation in experimental Parkinson's disease. Glia. 2010; 58(5):588–98. [PubMed: 19908287]
46. Rushmore TH, Morton MR, Pickett CB. The antioxidant responsive element. Activation by oxidative stress and identification of the DNA consensus sequence required for functional activity. J Biol Chem. 1991; 266(18):11632–9. [PubMed: 1646813]
47. Enomoto A, et al. High sensitivity of Nrf2 knockout mice to acetaminophen hepatotoxicity associated with decreased expression of ARE-regulated drug metabolizing enzymes and antioxidant genes. Toxicol Sci. 2001; 59(1):169–77. [PubMed: 11134556]
48. Nguyen T, et al. Nrf2 controls constitutive and inducible expression of ARE-driven genes through a dynamic pathway involving nucleocytoplasmic shuttling by Keap1. J Biol Chem. 2005; 280(37): 32485–92. [PubMed: 16000310]
49. Harman D. Aging: a theory based on free radical and radiation chemistry. J Gerontol. 1956; 11(3): 298–300. [PubMed: 13332224]
50. Martinez-Finley, EJ., et al. Free Radic Biol Med. 2013. Manganese neurotoxicity and the role of reactive oxygen species.
51. Hagen TM. Oxidative stress, redox imbalance, and the aging process. Antioxid Redox Signal. 2003; 5(5):503–6. [PubMed: 14580304]
52. Li J, Holbrook NJ. Common mechanisms for declines in oxidative stress tolerance and proliferation with aging. Free Radic Biol Med. 2003; 35(3):292–9. [PubMed: 12885591]
53. Kregel KC, Zhang HJ. An integrated view of oxidative stress in aging: basic mechanisms, functional effects, and pathological considerations. Am J Physiol Regul Integr Comp Physiol. 2007; 292(1):R18–36. [PubMed: 16917020]
54. Kim HL, Seo YR. Molecular and genomic approach for understanding the gene-environment interaction between Nrf2 deficiency and carcinogenic nickel-induced DNA damage. Oncol Rep. 2012; 28(6):1959–67. [PubMed: 23023193]
55. Yang B, et al. Deficiency in the nuclear factor E2-related factor 2 renders pancreatic beta-cells vulnerable to arsenic-induced cell damage. Toxicol Appl Pharmacol. 2012; 264(3):315–23. [PubMed: 23000044]
56. Dhakshinamoorthy S, Jaiswal AK. Functional characterization and role of INrf2 in antioxidant response element-mediated expression and antioxidant induction of NAD(P)H:quinone oxidoreductase1 gene. Oncogene. 2001; 20(29):3906–17. [PubMed: 11439354]
57. Itoh K, et al. An Nrf2/small Maf heterodimer mediates the induction of phase II detoxifying enzyme genes through antioxidant response elements. Biochem Biophys Res Commun. 1997; 236(2):313–22. [PubMed: 9240432]
58. Suh JH, et al. Decline in transcriptional activity of Nrf2 causes age-related loss of glutathione synthesis, which is reversible with lipoic acid. Proc Natl Acad Sci U S A. 2004; 101(10):3381–6. [PubMed: 14985508]
59. Zimmer B, et al. Sensitivity of dopaminergic neuron differentiation from stem cells to chronic low-dose methylmercury exposure. Toxicol Sci. 2011; 121(2):357–67. [PubMed: 21385734]
60. Itier JM, et al. Parkin gene inactivation alters behaviour and dopamine neurotransmission in the mouse. Hum Mol Genet. 2003; 12(18):2277–91. [PubMed: 12915482]

61. Berman SB, Zigmond MJ, Hastings TG. Modification of dopamine transporter function: effect of reactive oxygen species and dopamine. J Neurochem. 1996; 67(2):593–600. [PubMed: 8764584]

62. Chen R, et al. Direct evidence that two cysteines in the dopamine transporter form a disulfide bond. Mol Cell Biochem. 2007; 298(1–2):41–8. [PubMed: 17131045]

63. Johansson C, et al. Neurobehavioural and molecular changes induced by methylmercury exposure during development. Neurotox Res. 2007; 11(3–4):241–60. [PubMed: 17449462]

64. Barker DJ. The fetal origins of diseases of old age. Eur J Clin Nutr. 1992; 46(Suppl 3):S3–9. [PubMed: 1425543]

65. Barker DJ. Fetal origins of coronary heart disease. BMJ. 1995; 311(6998):171–4. [PubMed: 7613432]

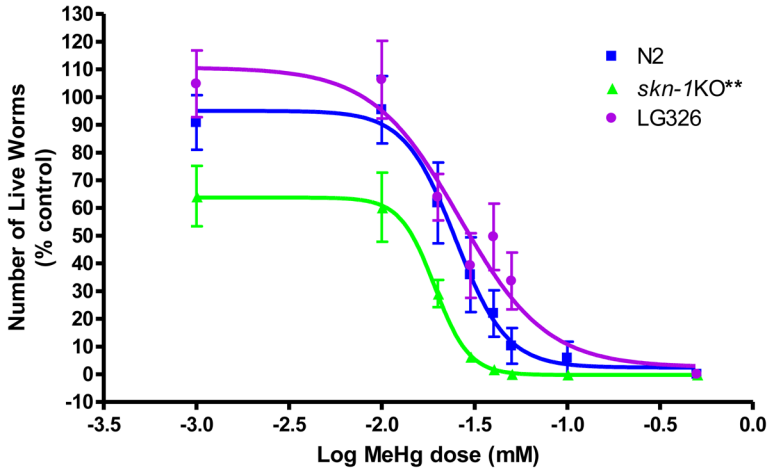

Figure 1.

Dose-response curve for MeHg-induced lethality in N2 wildtype and *skn-1*KO worms was used to determine appropriate doses for the remainder of the experiments Worms were exposed to MeHg in early-life (L1 stage) for 30 minutes and counted 24 hours following exposure. *skn-1*KO worms (LD_{50}= 19 μM, n=7) were more sensitive to MeHg than N2 wildtype worms (LD_{50} for N2 = 25 μM; n=8). LG326, in which *skn-1* is linked to GFP, (*skn-1*::GFP) had an LD_{50} = 26 μM; n=10.

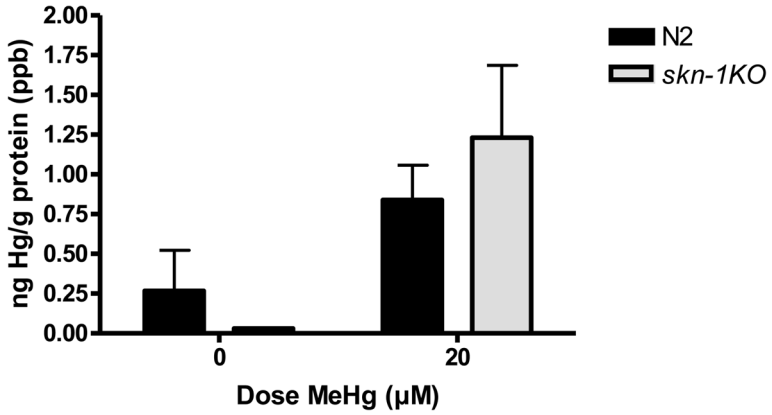

Figure 2.

Hg content in wildtype and *skn-1*KO worms. There was a significant increase in Hg content in MeHg exposed worms, as measured by ICP-MS, yielding a significant dose effect (*p=0.0003). Hg content was indistinguishable between N2 wildtype and *skn-1*KO strains. Results are presented as mean ± SEM of 4–5 independent experiments.

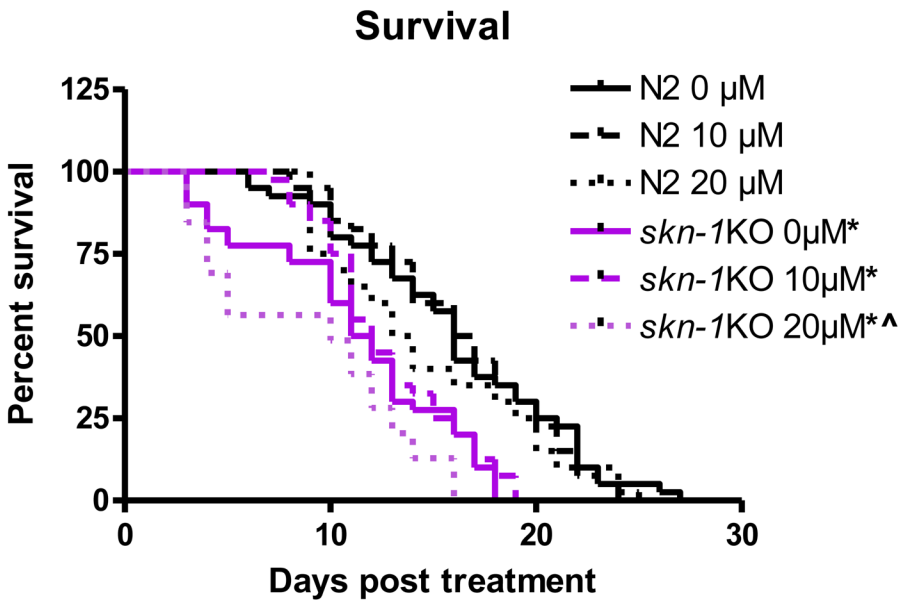

Figure 3.

Lifespan is affected in *skn-1*KO but not wildtype worms after early life exposure to MeHg. N2 wildtype worms do not show a decrease in lifespan following MeHg exposure. *skn-1*KOs exhibit reduced lifespan overall (compared to wildtype worms) (*$p<0.05$) with a further reduction in lifespan following 20 μM MeHg exposure (^$p=0.006$). Plotted values represent averages of three independent experiments, and the curves represent the best sigmoidal fit using log-rank statistics.

A.

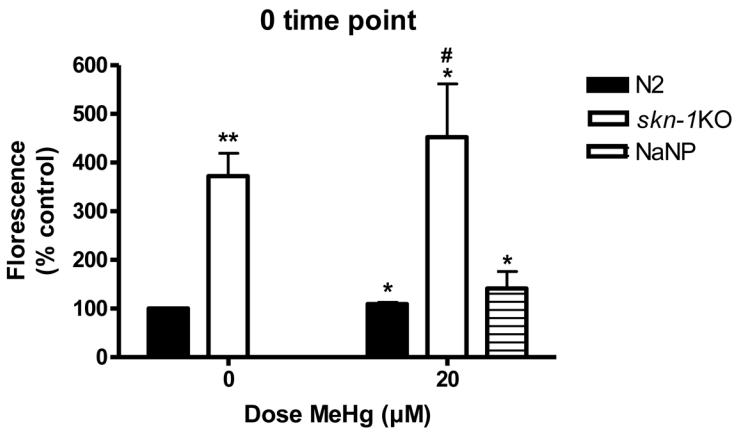

B.

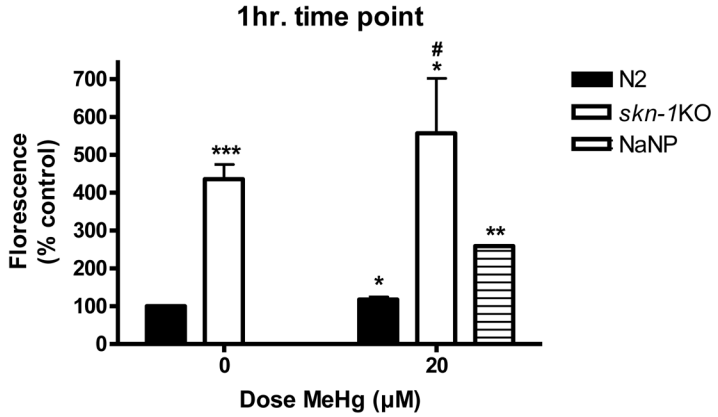

Figure 4.

Reactive oxygen species (ROS) levels are elevated in *skn-1*KOs and in N2 wildtype worms following early life MeHg exposure. (A) Immediately following MeHg exposure. Wildtype worms exhibit significantly higher ROS upon MeHg exposure (*p=0.04). Both untreated and treated *skn-1*KO worms (**p=0.0012;*p=0.018, respectively) show significant increase in ROS production compared to N2 wildtype untreated worms. *skn-1*KO MeHg treated worms are not significantly different from their respective untreated controls (p=0.5262, n.s.). *denotes significance from 0μM MeHg N2 wildtype (*p<0.05). #denotes significance from N2 wildtype 20 μM MeHg (#p<0.05). (B) One hour after 30 min MeHg exposure. Wildtype worms exhibit significantly higher ROS 1hr following MeHg exposure (*p=0.04). Both untreated and treated *skn-1*KO worms (***p=0.0001;*p=0.02, respectively) have significant ROS compared to wildtype untreated 1 hr following 30 minute early life exposure. *skn-1*KO MeHg treated worms were not significantly different from their respective untreated controls (p=0.4517, n.s.). NaNP=sodium nitroprusside (500μM) used as a positive control was significantly different from the 0 μM MeHg control (**p=0.002). *denotes significance from 0 μM MeHg wildtype (*p<0.05). #denotes significance from wildtype *2*0 μM MeHg (#p<0.05).

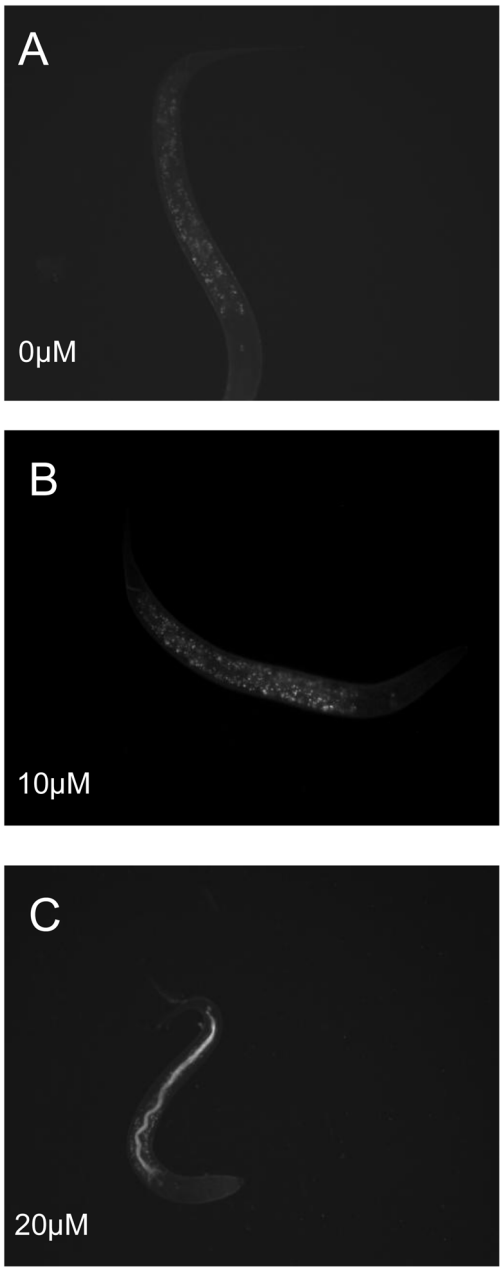

Figure 5.
SKN-1 induction in the gut following early life exposure to MeHg. LG326 worms (*skn-1*::GFP) were exposed to MeHg to visualize SKN-1 protein induction. SKN-1 expression in the gut can be seen in the 20 μM MeHg exposure group 24 hrs following exposure.

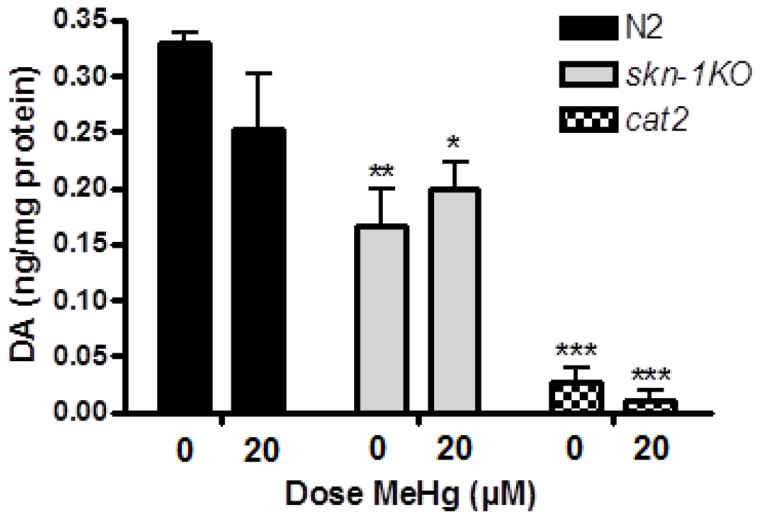

Figure 6.

DA levels are decreased in *skn-1*KO compared to N2 wildtype worms following early life exposure to MeHg. Total DA levels were measured by HPLC immediately following 30 min early life MeHg exposure (L1 stage). There was a significant difference between the 0 μM MeHg N2 wildtype worms and all other strains/doses (*p<0.05;**p<0.005;***p<0.0001). All doses and strains were significantly different from *cat-2*s (tyrosine hydroxlase deficient worms; used as a control).

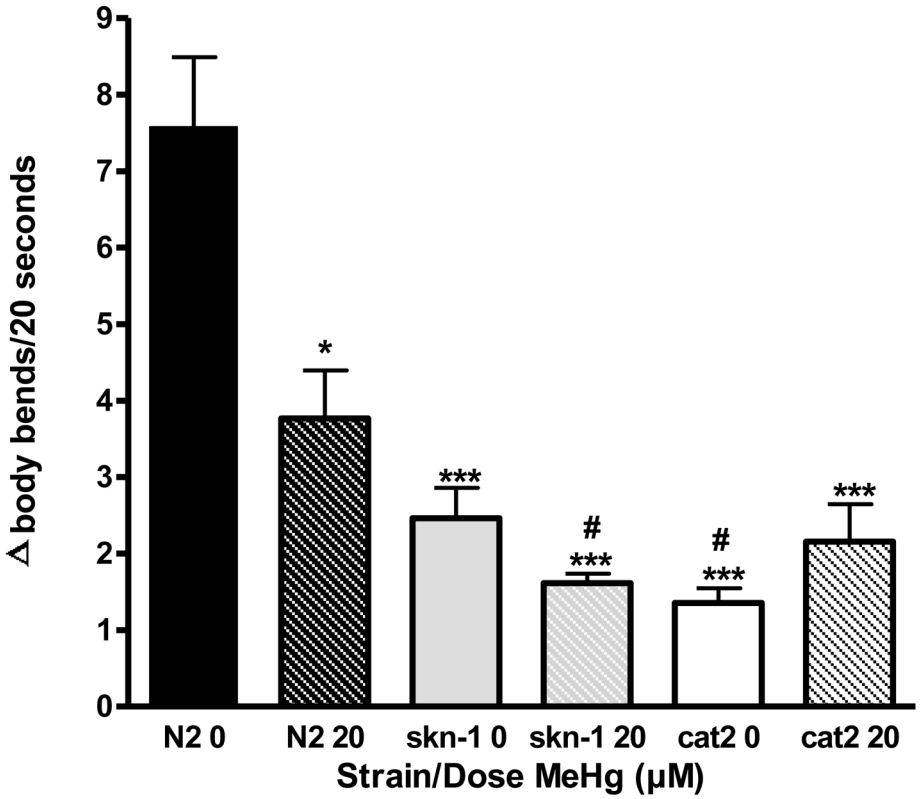

Figure 7.

MeHg has an effect on DA function as shown by the Basal Slowing Response. Loss-of-function of DAergic neurons is present later in life (72 hrs) following a single, early-life (L1 stage) exposure to 20μM MeHg. For each strain, locomotion rates in the absence and presence of bacteria (supplemental fig. 2) were calculated, and results are presented as change (Δ) body bends/20 seconds. Higher values indicate functional, while lower values indicate dysfunctional DAergic neurons. *cat-2* mutants (TH deficient) unexposed worms were significantly different from all MeHg-treated wildtype worms (*$p<0.05$). **denotes significance from 0μM MeHg N2 wildtype control (*$p<0.05$, ***$p<0.0005$). $^{\#\#}$ denotes significance from 0μM *skn-1*KO ($^{\#}p<0.05$). Error bars represent the mean ± SEM of 25–35 individual worms.

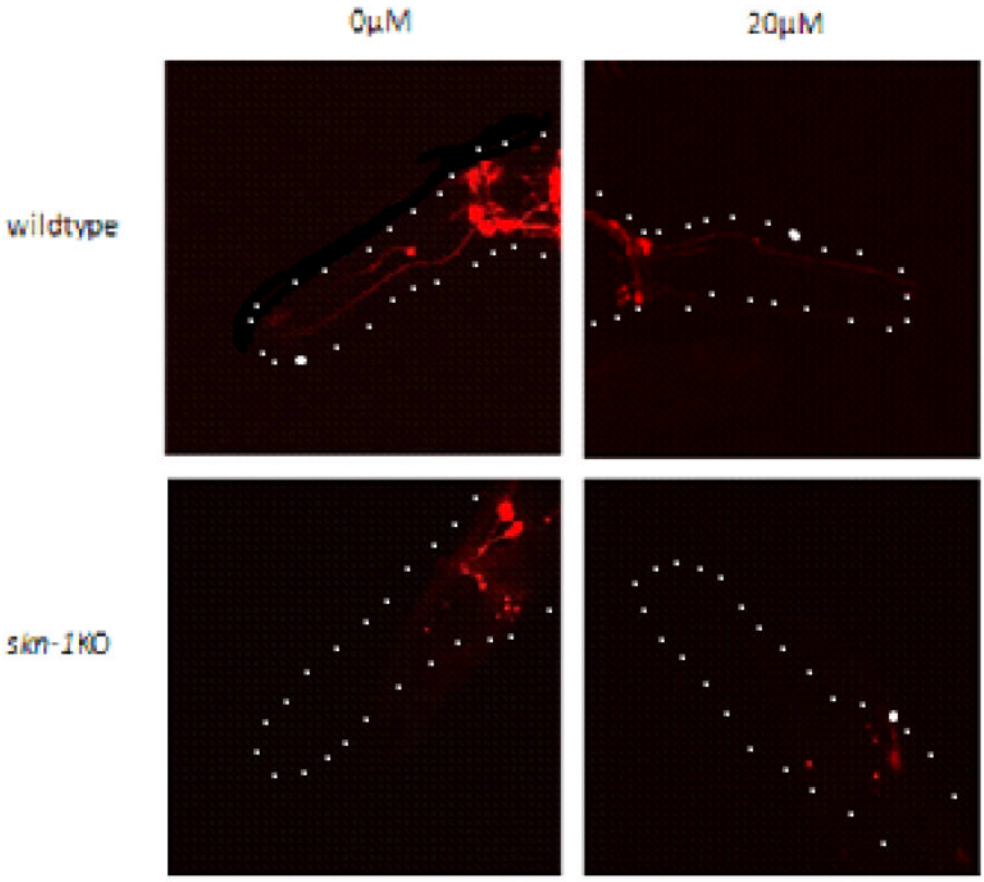

Figure 8.

Degeneration of DAergic neurons and loss of fluorescence are visible in *skn-1*KOs and treated N2 wildtype worms later in life (96 hrs) following a single early-life MeHg exposure. DAergic neurons, labeled with mCherry, in N2 wildtype and *skn-1*KO worms following exposure to 0 or 20 μM MeHg. CEP: cephalic (from nerve ring to tip of nose), ADE: anterior deirid DAergic neurons.